(6)

Satellite imagery analysis for nighttime temperature inversion clouds

K. Kawamoto, P. Minnis, R. Arduini and W. Smith, Jr.

Abstract

Clouds play important roles in the climate system. Their optical and microphysical properties, which largely determine their radiative property, need to be investigated. Among several measurement means, satellite remote sensing seems to be the most promising. Since most of the cloud algorithms proposed so far are daytime use which utilizes solar radiation, Minnis et al. (1998) developed a nighttime use one using 3.7-, 11- and 12-μm channels. Their algorithm, however, has a drawback that is not able to treat temperature inversion cases. We update their algorithm, incorporating new parameterization by Arduini et al. (1999) which is valid for temperature inversion cases. This updated algorithm has been applied to GOES satellite data and reasonable retrieval results were obtained.

1. Introduction

Regardless of the importance of clouds in the formation of the Earth's climate, its quantitative understanding is yet to be done. One of the important properties of clouds is the radiative property, which is determined by the optical depth, droplet size, top temperature and so on. To determine these cloud physical properties accurately is crucial, and it would lead to contribution of improvement for cloud processes, which are not fully resolved, in numerical models such as GCM (General Circulation Model).

Determination of cloud physical parameters using remote sensing techniques has been conducted actively during the last decade. (e.g., Nakajima et al. 1991) In particular satellite remote sensing is promising in view of large spatial coverage and constant temporal resolution. (e.g., Han et al. 1994) Most cloud retrieval algorithms have been constructed only for daytime and require solar spectral channels. Except for CO2-slicing methods, techniques applicable to nighttime are rare because fewer wavelengths are available. Since a consistent 24-hour retrieval of cloud properties is indispensable for studies of cloud diurnal variability, the hydrological cycle and cloud-radiation interactions, a nighttime cloud algorithm using common infrared spectral channels has been developed for application to both research and operational meteorological satellites. Our method makes use of brightness temperature difference (BTD) for determining the optical depth, droplet size and temperature of clouds (Inoue, 1985, Minnis et al. 1995). Minnis et al. (1998) developed parameterization for reflectance and effective emittance of clouds in order to treat huge satellite data set efficiently. Their parameterizations are, however, only valid under the condition of the brightness temperature at cloud base, Ts minus the cloud temperature, $Tc > 4$K. Then Arduini et al. (1999) constructed a parameterization for brightness temperature (BT) of clouds under the condition of Ts-$Tc < 4$K. This temperature range covers fog or temperature inversion clouds, which are particularly common in polar regions. In this article, we will report a case study with our nighttime cloud algorithm which incorporated Arduini et al's parameterization In section 2, retrieval principles of our method and Arduini et al's parameterization will be described, and in section 3 satellite data and some other sounding data will be presented. We will summarize results in the final section.

2. Method

1) Retrieval principles

The Solar-infrared Infrared Split-window Technique (SIST) uses 3.7-, 11- and 12-μm channels to invert three cloud parameters, that is, the optical depth τ, effective water droplet radius re or effective ice particle diameter De and temperature Tc of both water and ice clouds. Because of little sensitivity of the particle size, we limit our analysis to clouds whose optical thicknesses less than 6. In principle, these parameters can be determined by matching BTDs between observation and model calculation as closely as possible. The parameterization to calculate modeled BT will be presented in the next subsection Meteorological data such as temperature, isobaric height and relative humidity are taken from the nearest sounding data. Water vapor absorption is based on the correlated k-distribution by Kratz (1995).

The analysis flow is as follows. In one particle model, τ is determined at a given *Tc* so as to generate the modeled BT at 11-μm as closely as possible to the observed counterpart, and then error between observed and modeled BTDs which τ and *Tc* produce is calculated. We search *Tc* which produces the minimum BTD error by bisection method between BT at 11-μm and the maximum sounding temperature. This procedure is done for both water and ice models, and then the pair of τ, *re* or *De* and *Tc* which results in smaller BTD error between both phases is taken as solution. Phase selection is, however, taken into account in some particular conditions. For example, ice will be selected if *Tc* (ice) < 243K, or if both *Tc* (water) and *Tc* (ice) < 253K, or if *Tc* (water) < 273K and *re* < 2.5μm. Water will be selected if *Tc* (water) > 270K and *Tc* (ice) > 265K.

2) cloud-top BT parameterization for temperature inversion situations

To model the brightness temperatures (BT) of clouds, Arduini et al. (1999) developed its parameterization under the condition of *Ts*-*Tc* < 4K, that is, the cloud temperature is warmer than or similar to that of the underlying layer. It is functions of τ, *re* and *De*, viewing zenith angle, *Tc* and *Ts*, and τ covers from 0.25 to 32, *Tc* ranges from 240K to 300K and viewing zenith angle is up to 78 degrees. Water-droplet clouds were represented by using modified Gamma distribution of spherical droplets having *re* from 2μm to 32μm. On the other hand, ice-crystal clouds were assumed to be made up of distributions of hexagonal ice crystals whose optical properties were based on the ray-tracing results of Takano and Liou (1989) and the spheroidal approximation of Takano et al. (1992). *De* ranges from 6μm to 135μm.

An adding-doubling radiative transfer code was used to simulate cloud-top BT, and then a standard linear least squares multiple regression technique, which is similar to that of Minnis et al. (1998), was taken to analyze the model results and to determine the parameterization. Results show that this parameterization successfully describes the variation in the temperature with the root mean square of the residuals well within 0.5K.

3. Data

In this work, we use GOES (Geostationary Operational Environmental Satellite) data over Oklahoma on Oct. 26 1995. Well-defined fog developed in the northern Oklahoma on that day. This area is suitable for validating the present algorithm, since some ground measurements were conducted at ARM (Atmospheric Radiation Measurement) site (36.6N, 97.5W).

Figure 1 shows the GOES IR (11-μm) imagery. Area enclosed by square, where is darker than surroundings (it means warmer than nearby ordinary clouds), corresponds the fog involved in this paper.

4. Result and concluding remarks

We analyzed the area indicated in Fig. 1 with the present algorithm. Figure 2 shows the parameterization result for BTD between 3.7-μm and 11-μm as a function of BT at 11-μm with regard to several values of τ and *re*, together with observation points superimposed. In this example, we set skin temperature as 281K taken from the nearest measurement point. The cloud height is retrieved about 0.8km, τ is retrieved about 0.4 to 1.2, and *re* is inferred 4 to 12μm. As for the cloud height, lidar at ARM site indicates similar values to ours. Air temperature and dew-point temperature vertical profiles from the sounding also support our retrievals as shown in figure 3. Such a type of cloud occurs near the temperature inversion height in general, and humidity is also found to be enhanced. As for *re*, these values seem to be consistent with those of continental low clouds. In addition, surface observers reported no drizzle which usually associated with larger droplets.

In particular, it might be very sensitive to input temperatures for remote sensing techniques using infrared channels like the present algorithm. We present another computation using the parameterization with different skin temperature input in figure 4. We set it as 275K in this case. Then *re* would be retrieved as much larger and we would get totally wrong results. It clearly shows how it is important to use accurate temperatures.

In this paper, we have incorporated cloud BT parameterization for temperature inversion cases by Arduini et al. (1999) to the nighttime cloud analysis framework by Minnis et al. (1995). This new cloud analysis system has been applied to low-level clouds found in GOES satellite imagery over Oklahoma. Our retrieval for the cloud height is consistent with the lidar result and sounding. As for *re*, the values seem to be reasonable. This algorithm would be a powerful tool for global analysis and statistical study of clouds, together with the one with Minnis et al. (1998).

References

Arduini R. F., P. Minnis and D. F. Young, 1999: Parameterization of cloud-top brightness temperature at solar-IR and IR wavelengths for low clouds and fog. Proc. AMS 10th Conf. Atmos. Rad.,Madison, WI, June 28-July 2.

Han, Q.,W. B. Rossow and A. A. Lasis, 1994: Near-global surbey of effective droplet radii in liquid water clouds using ISCCP data. *J. Climate*, **7**, 465-497

Inoue, T., 1985: On the temperature and effective emissivity determination of semi-transparent cirrus clouds by bi-spectral measurements in the 10 μm region. *J. Meteor. Soc. Japan*, **63**, 88-98.

Kratz, D. P., 1995: The correlated k-distribution as applied to the AVHRR channels. *J. Quant. Spectrosc. Radiat. Transfer*, **53**, 501-507.

Minnis, P. and co-authors, 1995, Cloud and the Earth's Radiation Energy Sysem(CERES) Algorithm Theoretical Basis Document, NASA Reference Publication 1376, volume III, pp242

Minnis, P., D. P. Garber, D. F. Young, R. F. Arduini and Y. Takano, 1998: Parameterization of reflectance and effective emittance for satellite remote sensing of cloud properties. *J. Atmos. Sci.*, **55**, 3313-3339

Nakajima, T., M. D. King, J. D. Spinhirne and L. F. Radke, 1991: Determination of the optical thickness and effective radius of clouds from reflected solar radiation measurements. Part II: Marine stratocumulus observations. *J. Atmos. Sci.*, **48**, 728-750.

Takano, Y. and K.-N. Liou, 1989: Radiative transfer in cirrus clouds: I. Single scattering and optical properties of oriented hexagonal ice crystals. *J. Atmos. Sci.* **46**, 3-20.

Takano, Y., K.-N. Liou and P. Minnis, 1992; The effects of small ice crystals on cirrus radiative properties. *J. Atmos. Sci.* **49,** 1487-1493.

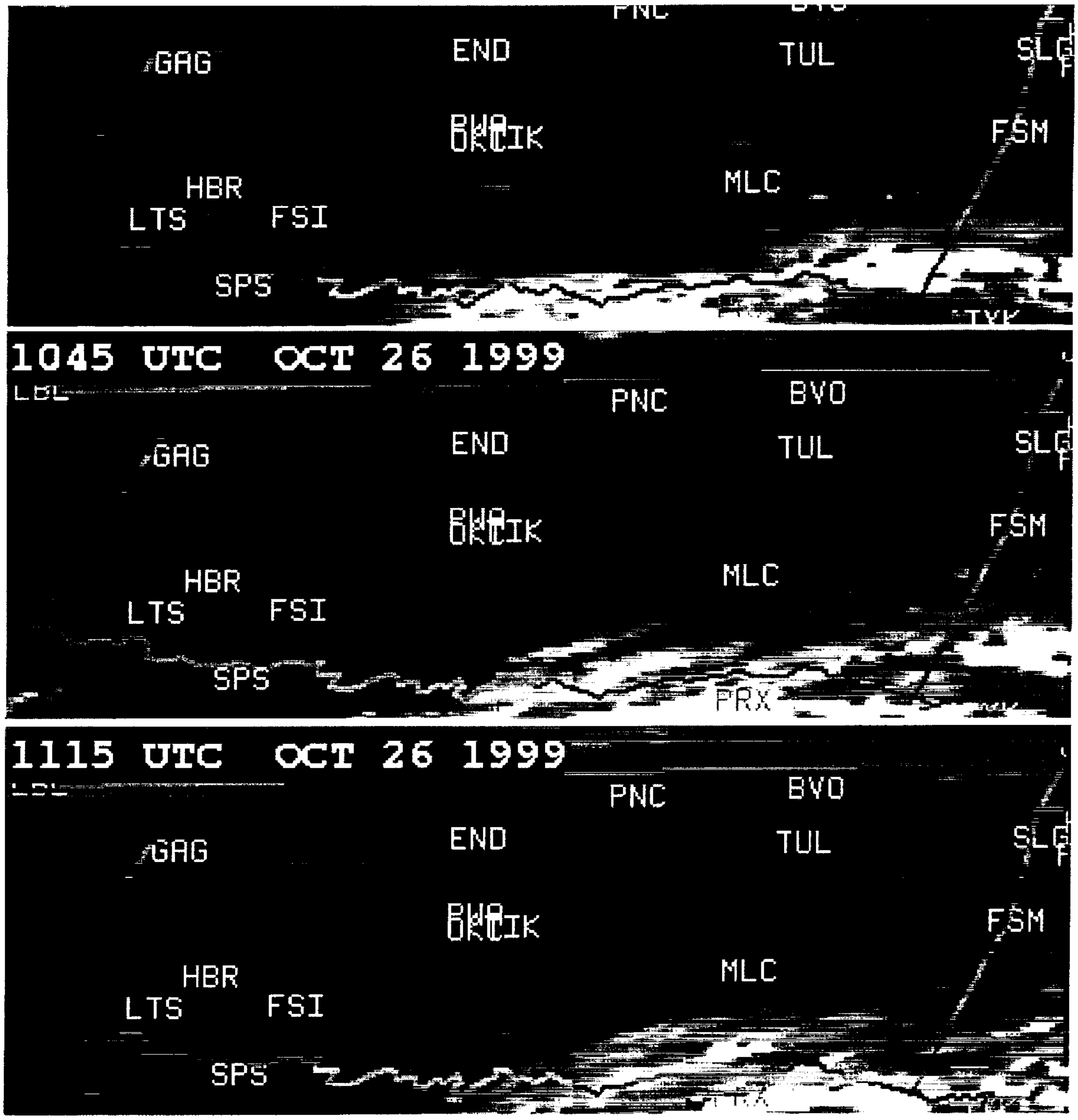

fig. 1

	Day	Time hhmm	StCo	Sta id	T [F]	Td [F]	Dir	Spd [kts]	Gus	AltSet [mb]	Vis [mi]	Weather	Ceil
	26	0857	OKUS	GAG	34	28	270	5		1009.2	15.00		0/
	26	1052	OKUS	GAG	35	29	260	6		1007.8	15.00		0/
GAGE	26	1154	OKUS	GAG	40	33	000	0		1007.5	15.00		
FC OBS	26	1257	OKUS	GAG	47	37	000	0		1005.8	15.00		8/007
	26	1352	OKUS	GAG	46	35	260	7		1005.8	15.00		8/007
	26	1456	OKUS	GAG	49	41	250	6		1004.1	8.00		8/005
	26	1553	OKUS	GAG	56	45	210	10		1002.4	15.00		
	26	0955	OKUS	END	48	42	130	7		1008.8	7.00		
	26	1055	OKUS	END	48	42	100	6		1008.1	7.00		
ENID	26	1155	OKUS	END	47	42	080	7		1007.8	7.00		
FC OBS	26	1255	OKUS	END	46	43	090	8		1006.4	6.00	F	
	26	1355	OKUS	END	47	43	120	8		1005.8	7.00		5/031
	26	1500	OKUS	END									
	26	1555	OKUS	END	59	52	210	10		1003.4	6.00	F	5/007
	26	0952	OKUS	PNC	50	45	000	0		1010.2	12.00		0/
	26	1057	OKUS	PNC	50	46	000	0		1009.5	12.00		8/030
nca City	26	1152	OKUS	PNC	53	47	170	7		1008.5	12.00		8/030
FC OBS	26	1253	OKUS	PNC	54	48	160	8		1007.5	12.00		8/025
	26	1354	OKUS	PNC	55	48	140	8		1006.4	12.00		5/025
	26	1453	OKUS	PNC	57	49	140	9		1005.1	12.00		5/250
	26	1558	OKUS	PNC	60	53	190	8		1003.7	12.00		5/012

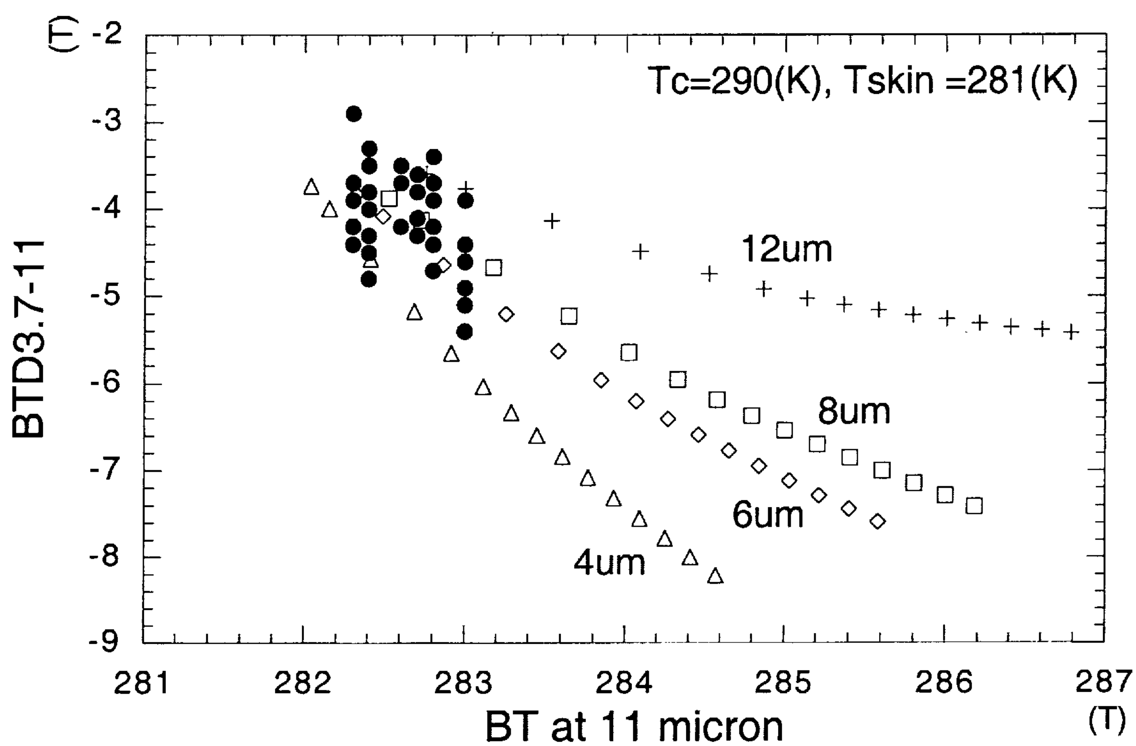

Tc=290(K), Tskin =281(K)
12um
8um
6um
4um
BTD3.7-11
(T)
BT at 11 micron
(T)
281
282
283
284
285
286
287
-2
-3
-4
-5
-6
-7
-8
-9

fig. 2

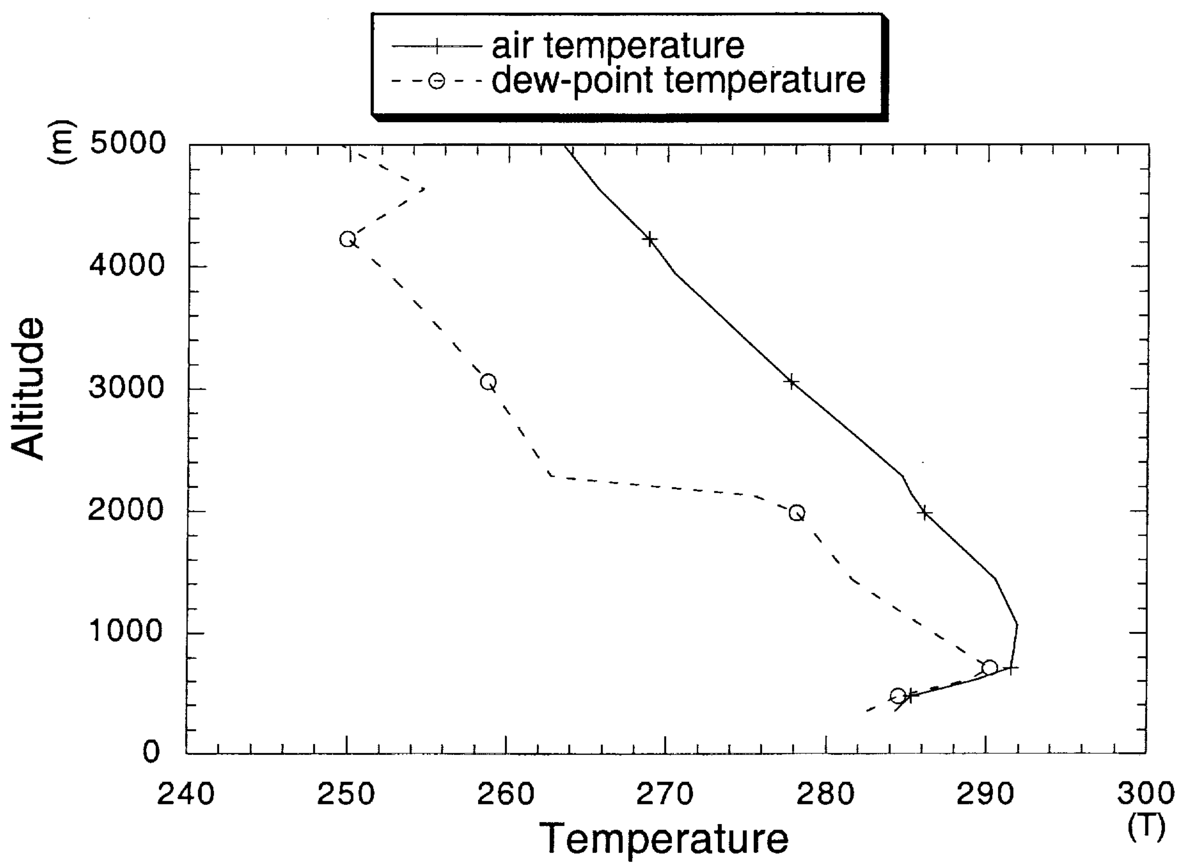
air temperature
dew-point temperature
(m)
5000
4000
3000
2000
1000
0
Altitude
240
250
260
270
280
290
300
(T)
Temperature

fig. 3

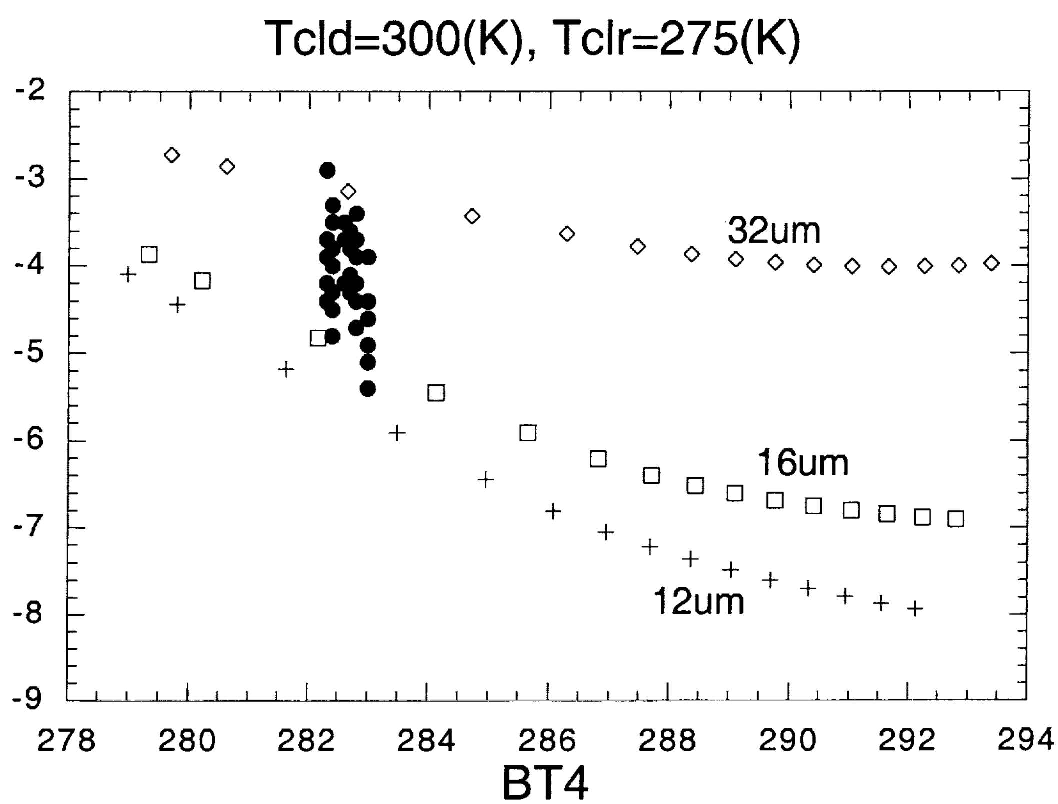

Tcld=300(K), Tclr=275(K)
-2
-3
-4
-5
-6
-7
-8
-9
278
280
282
284
286
288
290
292
294
BT4
32um
16um
12um

fig. 4